

Negative effective permeability and left-handed materials at optical frequencies

Andrea Alù^(1,2), Alessandro Salandrino^(1,2), and Nader Engheta^{(1),}*

*(1) University of Pennsylvania, Department of Electrical and Systems Engineering,
Philadelphia, PA, U.S.A., engheta@ee.upenn.edu*

*(2) University of Roma Tre, Department of Applied Electronics,
Rome, Italy, alu@uniroma3.it.*

Receipt date: December 9, 2004

Abstract

We show a design of nano-inclusions made of metallic nanospheres exhibiting a resonant magnetic dipole response in the near infrared and visible domain. When such inclusions are embedded in a host medium, they may provide metamaterials with negative effective permeability at optical frequencies. We also show how the same inclusions may provide resonant electric dipole response and, when combining the two effects at the same frequencies, left-handed materials with both negative effective permittivity and permeability may be synthesized in the optical domain.

PACS: 71.45.Gm, 78.20.-e, 73.20.Mf

* To whom correspondence should be addressed

The interest in materials with negative effective magnetic, as well as electric, properties has grown considerably in the past several years, mainly due to the recent interest in unconventional characteristics of composite *metamaterials* with both negative permittivity and permeability, also known as left-handed (LH) or double negative (DNG) materials [1]. In the microwave regime, such complex materials have been constructed by embedding arrays of metallic split-ring resonators (SRR) and wires in a host medium and some of their anomalous properties have been experimentally demonstrated [2]. In the near-infrared (IR) and visible regimes, however, synthesizing such LH materials faces certain challenges, since in these frequency regimes the magnetic permeability due to the molecular currents in a material tends to approach to the free space permeability [3], and the straightforward scaling of the metallic SRR down to the optical wavelength may encounter other related issues. Following these difficulties, several novel ideas have been put forward by other researchers to achieve LH materials in the IR and visible regimes. They include the possibility of using plasmonic parallel nanowires [4], modified split ring resonator in the near-IR region [5], closely-packed inclusions with negative permittivity and their electrostatic resonances [6], and defects in regular photonic band gap structures [7].

Here we present another approach to design sub-wavelength inclusions that exhibit magnetic dipolar resonant response, and thus provide the possibility of having negative effective magnetic dipole moment, at optical frequencies. The idea is based on the collective resonance of an array of plasmonic nanospheres arranged in a specific pattern (e.g., in a circular pattern) to form a single sub-wavelength “loop macro-inclusion”. In this loop, it is not the conventional conduction current (as in the SRR at microwaves) that produces the magnetic dipole moment, but instead it is the plasmonic resonant feature of every nanosphere that induces a circulating “displacement” current around this loop. Unlike the case of the conventional metallic loops or SRRs at the microwave frequencies, here the size of this loop does not directly influence the resonant frequency of the induced magnetic dipole moment, but rather the plasmonic resonant frequency of the nanoparticle is the main determining factor for this resonance to happen.

Consider N identical nanospheres with radius a arranged to have their centers located symmetrically on a circle of radius R , as depicted in Fig. 1. A Cartesian coordinate system (x, y, z) along with a related spherical coordinate system (r, θ, ϕ) is considered here. We assume $a \ll R \ll \lambda_0$, where λ_0 is the free space wavelength. The position vectors of these nanoparticles are described as:

$$\mathbf{r}_n = \hat{\mathbf{x}} \left[R \cos \left((n-1) \frac{2\pi}{N} \right) \right] + \hat{\mathbf{y}} \left[R \sin \left((n-1) \frac{2\pi}{N} \right) \right] = R \hat{\mathbf{r}}(\mathbf{r}_n), \quad (1)$$

with $n=1, 2, \dots, N$ and $\hat{\mathbf{r}}$ being the spherical radial unit vector.

In order to single out the magnetic response of this structure, we excite the system with the following system of N symmetrical plane waves (see e.g., [8]):

$$\mathbf{H}_0 = \hat{\mathbf{z}} \sum_{n=1}^N \frac{H_0}{N} e^{i\mathbf{k}_n \cdot \mathbf{r}}, \quad \mathbf{E}_0 = \sum_{n=1}^N \mathbf{E}_{0n} e^{i\mathbf{k}_n \cdot \mathbf{r}}, \quad (2)$$

with:

$$\begin{cases} \mathbf{k}_n = -k_0 \hat{\mathbf{r}}(\mathbf{r}_n) \\ \mathbf{E}_{0n} = -\frac{\eta_0 H_0}{N} \hat{\boldsymbol{\phi}}(\mathbf{r}_n) \end{cases}, \quad (3)$$

where μ_0 is the free space permeability, $k_0 = \omega \sqrt{\varepsilon_0 \mu_0}$ is the free space wave number, $\hat{\boldsymbol{\phi}}$ is the spherical azimuth unit vector and the impinging wave is assumed to be monochromatic with an $e^{-i\omega t}$ time dependence. Moreover, H_0 is the magnetic field amplitude at the origin produced by this combined excitation.

Since the nanospheres composing the loop are small compared to the wavelength and the distance between adjacent nanospheres is taken to be relatively large compared to their diameters, in the first-order approximation the interactions among the particles are well described by their induced electric dipole moments:

$$\mathbf{p}_n = \alpha \mathbf{E}_{loc}(\mathbf{r}_n) = p \hat{\boldsymbol{\phi}}(\mathbf{r}_n), \quad (4)$$

where α is the polarizability coefficient of the particles (which is scalar since the nanospheres are assumed to have an isotropic behavior) and $\mathbf{E}_{loc}(\mathbf{r}_n)$ is the local field at the n^{th} particle location (in the absence of that particle), given by the sum of the incident applied field and the fields scattered by all the other particles at that point. The last equality in (4) holds due to the symmetry of the geometry and of the excitation. In fact, as depicted in Fig. 1a, the symmetric excitation of Eq. (2) provides an almost uniform time-varying magnetic field around the inclusion, inducing electric dipole moments (due to Faraday's induction) on each nanoparticle that circulate around the axis of the magnetic field.

The local field $\mathbf{E}_{loc}(\mathbf{r}_n)$ may be written in the dyadic form:

$$\mathbf{E}_{loc}(\mathbf{r}_n) = \mathbf{E}_0(\mathbf{r}_n) + p \sum_{l \neq n}^N \underline{\mathbf{Q}}_{ln} \cdot \hat{\boldsymbol{\phi}}(\mathbf{r}_l), \quad (5)$$

where $\underline{\mathbf{Q}}_{ln}$ is the Green's dyad, as usually defined (see e.g., [9]). Combining (4) and (5) we get:

$$p = \frac{\mathbf{E}_0(\mathbf{r}_n) \cdot \hat{\boldsymbol{\phi}}(\mathbf{r}_n)}{\alpha^{-1} - \sum_{l \neq n}^N \underline{\mathbf{Q}}_{ln} \cdot \hat{\boldsymbol{\phi}}(\mathbf{r}_l) \cdot \hat{\boldsymbol{\phi}}(\mathbf{r}_n)}, \quad (6)$$

In the limit of $k_0 R \ll 1$, the electromagnetic far-zone fields scattered by such a configuration of nanoparticles are given by:

$$\begin{aligned} \mathbf{E} &\simeq -\frac{iNk_0^3 R}{8\pi\epsilon_0} \frac{e^{ik_0 r}}{r} p \sin \theta \hat{\boldsymbol{\phi}} \\ \mathbf{H} &\simeq \frac{iNk_0^3 R}{8\pi\epsilon_0 \eta_0} \frac{e^{ik_0 r}}{r} p \sin \theta \hat{\boldsymbol{\theta}} \end{aligned}, \quad (7)$$

which by inspection correspond to those radiated by an effective magnetic dipole with amplitude

$$\mathbf{m}_H = \frac{-i\omega p N R}{2} \hat{\mathbf{z}}. \quad (8)$$

It may be verified that the quasi-static multipole expansion of the current distribution

$$\mathbf{J}_H = \sum_{n=1}^N -i\omega \mathbf{p}_n \delta(\mathbf{r} - \mathbf{r}_n) \text{ yields to a magnetic dipole moment consistent with (8), ensuring,}$$

moreover, that electric dipole moments up to the order $N - 1$ and even-order magnetic moments up to the order N are identically zero. The other non-vanishing higher-order electric and magnetic multipoles are respectively proportional in amplitude to $(k_0 R)^{m-1}$ and $(k_0 R)^m$, where $m > N$.

The relative strength of the higher-order multipoles provides an insight into how closely packed we may embed many such nano-loops in a host medium in order to form a bulk medium with magnetic properties. It is clear that, by increasing N and/or decreasing $(k_0 R)$, more higher-order multipoles may be canceled or diminished, and therefore the ratio between the non-vanishing higher-order multipole amplitudes and the magnetic dipole moment may be made sufficiently small to be neglected.

The magnetic polarizability α_{mm} of the nano-loop, which relates the induced magnetic dipole moment to the excitation field through $\mathbf{m}_H = \alpha_{mm} \mathbf{H}_0(\mathbf{0})$, can be calculated from (8) and (6). In the limit of $k_0 R \ll 1$, its expression is written in closed form as:

$$\alpha_{mm}^{-1} = \frac{4\varepsilon_0}{Nk_0^2 R^2} \alpha^{-1} - i \left(\frac{k_0^3}{6\pi} - \frac{2k_0}{3\pi N R^2} \right) + \frac{1}{16\pi N k_0^2 R^5} \sum_{l \neq n}^N \frac{3 + \cos[2\pi(l-n)/N]}{|\sin[\pi(l-n)/N]|^3}. \quad (9)$$

For a small homogeneous isolated single nanosphere of permittivity ε the expression for α may be given as [10]:

$$\alpha = \left[\left(4\pi\varepsilon_0 a^3 \frac{\varepsilon - \varepsilon_0}{\varepsilon + 2\varepsilon_0} \right)^{-1} - i \frac{k_0^3}{6\pi\varepsilon_0} \right]^{-1}. \quad (10)$$

As evident from (9), the magnetic polarizability may hit the resonance for values close to the resonance of the single nanosphere electric polarizability, which happens at frequencies for which $\varepsilon \simeq -2\varepsilon_0$. In particular, the resonance in (9) is slightly shifted along the frequency axis with respect to (10), due to the coupling term represented by the summation.

As long as the loop macro-particle is small compared to the wavelength ($k_0 R \ll 1$) and therefore (9) is valid and describes sufficiently well the electromagnetic properties of the “loop” particle, it

is possible to embed many such loops in a host medium in order to synthesize a composite material with resonant magnetic properties at optical frequencies. The effective permeability of such a composite can be obtained using the effective medium theory for a case of randomly located macro-particles and for a case of 3-D periodic arrangement of such particles [11], and is expressed as:

$$\mu_{eff}^{(r)} = \mu_0 \left(1 + \frac{1}{N_d^{-1} \alpha_{mm}^{-1} - 1/3} \right), \quad \mu_{eff}^{(p)} = \mu_0 \left(1 + \frac{1}{N_d^{-1} [\alpha_{mm}^{-1} + i(k_0^3/6\pi)] - 1/3} \right), \quad (11)$$

for the random distribution and the regular 3-D periodic distribution of loops, respectively. Here N_d is the number density of loop macro-particles per unit volume.

Fig. 2 shows, as examples, the behavior of $\mu_{eff}^{(p)}$ for two periodic lattices designed to exhibit a negative permeability in the near IR. The loops have been designed using silver nanospheres with the appropriate Drude model for their permittivity in this frequency range [12]. Realistic material loss has been included in this analysis. It is worth noting how the magnetic resonance is appreciable over a relatively wide range of frequencies. For a higher number of spheres per loop the resonance is generally stronger, as clearly evident by comparing Figs. 2a and 2b, even though the resonance may shift in frequency.

Similar results may be obtained by removing the hypothesis of isotropic particles that form the loop. For symmetry reasons, in fact, following the previous analysis, we may employ anisotropic particles (e.g., ellipsoids, nanorods, nanodiscs), provided that their relative orientation is parallel to $\hat{\phi}(\mathbf{r}_n)$. This may provide further degrees of freedom to allow designing a bulk material with magnetic response having the resonance at a desired frequency.

The electric response of the nano-inclusion of Fig. 1 may be calculated in an analogous way. This time the composed excitation should be:

$$\begin{aligned}\mathbf{E}_0 &= E_0 \cos(k_0 x) \hat{\mathbf{y}} \\ \mathbf{H}_0 &= \frac{iE_0 \sin(k_0 x)}{\eta_0} \hat{\mathbf{z}},\end{aligned}\tag{12}$$

which corresponds to having two symmetric, counter-propagating plane waves added together in phase at the origin, in order to isolate the electric response of the inclusion. For small enough loops, the induced total electric dipole moment will be proportional to the electric polarizability α_{ee}^y of the loop. As will be seen below, due to the lack of symmetry, the loop exhibits an anisotropic response for its electric polarizability even in the x-y plane. By increasing the number N of nano-particles composing the loop, however, this planar anisotropy diminishes.

The dipole moment induced on the n -th sphere may be evaluated through the vectorial relation:

$$\mathbf{p}_n = \alpha \mathbf{E}_{loc} = \alpha \left[\mathbf{E}_0(\mathbf{r}_n) + \sum_{l \neq n}^N \mathbf{Q}_{ln} \cdot \mathbf{p}_l \right].\tag{13}$$

A system of N equations (13), for $n=1..N$, may be solved numerically to derive the induced dipole moments \mathbf{p}_n . In the limit of $k_0 R \ll 1$, the multipole expansion of such a distribution is dominated by the effective dipole moment $\mathbf{p}_E^{(1)} = \sum_{n=1}^N \mathbf{p}_n$, which due to the symmetry is parallel to the applied field \mathbf{E}_0 . The induced dipole distribution for this case is sketched in Fig. 1b. The related polarizability factor α_{ee}^y , which satisfies the relation $\mathbf{p}_E = \alpha_{ee}^y \mathbf{E}_0(\mathbf{0})$, may be straightforwardly calculated numerically and analogous results may be obtained for the quantity α_{ee}^x , for an electric field excitation polarized along $\hat{\mathbf{x}}$. The two quantities are expected to be the same for N being a multiple of 4, and increasingly more similar for higher values of N .

The effective permittivity for the bulk medium is given by the following expressions, analogous to (11):

$$\varepsilon_{eff}^{(r)} = \varepsilon_0 \left(1 + \frac{1}{\varepsilon_0 N_d^{-1} \alpha_{ee}^{-1} - 1/3} \right), \quad \varepsilon_{eff}^{(p)} = \varepsilon_0 \left(1 + \frac{1}{\varepsilon_0 N_d^{-1} [\alpha_{ee}^{-1} + i(k_0^3 / 6\pi \varepsilon_0)] - 1/3} \right).\tag{14}$$

Fig. 3 reports the effective permittivity calculated for the same composite media simulated in Fig. 2. It is interesting to note how for a larger number of spheres per loop it is possible to achieve significant double resonances, as in Fig. 3a. The dotted lines in the figures represent the effective permittivity of another composite medium that could be formed by embedding the same number density of nanospheres when these spheres are dispersed in a regular periodic lattice, not collected in loops as in our case. As can be seen, as the number of spheres per loop increases, the two curves become more different, since this loop effect become more pronounced.

It is important to point out how the metamaterial synthesized in Fig. 2b and 3b shows a range of frequency in the near IR in which both effective permittivity and permeability have negative real parts simultaneously. This happens since the small number of spheres per loop (four in the example) does not sensibly shift the resonance position along the frequency axis for the magnetic permeability. Therefore the two resonances happens around the plasmonic resonance of the single nanospheres (around $\varepsilon = -2\varepsilon_0$) This overlapping of the two resonances provides us with the possibility to synthesize an effective double-negative (or LH) material in the near IR. The results are reported in Fig. 4, where the effective index of refraction is plotted as a function of frequency. We notice how there is a range of frequency in which this metamaterial may have negative refraction with reasonably low losses.

As a final example, we have designed a similar layout to work in the visible regime. The results for the expected effective permeability and permittivity are reported in Fig. 5. The plots show the results with and without considering the real losses of silver in the visible regime, where the constitutive parameters of silver have now been interpolated from real experimental data [13] in the range of frequency of the visible light. Notice how the higher losses of silver in this frequency range eventually affect the resonance of the structure, particularly for the magnetic resonance. When losses are neglected, the proposed effect can be clearly seen, but when real loss for silver is considered, the resonant effect is considerably weaker, and the effective permeability does not

reach negative values in this example. The geometry of the single inclusions and their material, however, may be adjusted to achieve in principle a stronger resonance also at these frequencies following the same principle.

This work was supported in parts by the U.S. Defense Advanced Research Projects Agency (DARPA) Grant number HR0011-04-P-0042 and by the U.S. Air Force Office of Scientific Research (AFOSR) Grant number F49PRE-03-1-0438. Andrea Alù has been partially supported by the 2004 SUMMA Graduate Fellowship in Advanced Electromagnetics.

FIGURES

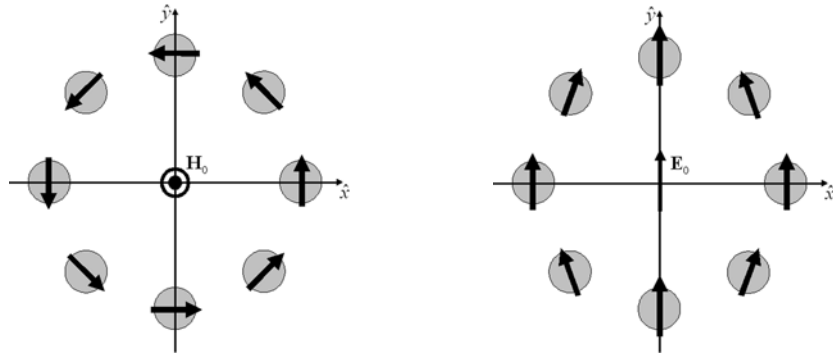


Fig. 1 – A circular array of equi-spaced nanospheres in the x - y plane excited by: a) a local time-varying magnetic field directed along z ; b) a local time-varying electric field directed along y . The vectors on each particle indicate the induced electric dipole moments in the two cases.

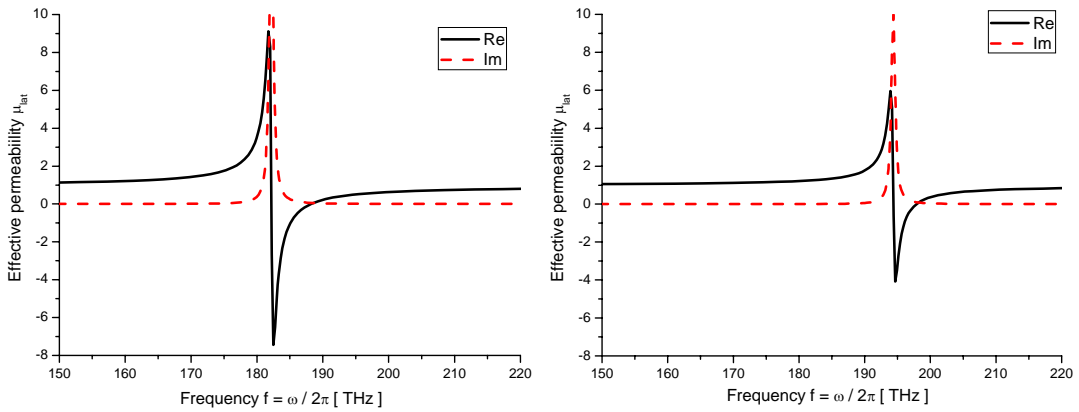


Fig. 2 – Effective relative magnetic permeability $\mu_{\text{eff}}^{(p)} / \mu_0$ for bulk media with the following parameters for the geometry of nano-inclusion: a) $R = 377 \text{ nm}$, $a = 125 \text{ nm}$, $N = 6$, $N_d = (1.13 \mu\text{m})^{-3}$; b) $R = 188 \text{ nm}$, $a = 62.5 \text{ nm}$, $N = 4$, $N_d = (556 \text{ nm})^{-3}$. Following [12], in this range of frequency the permittivity of silver has been assumed to follow the Drude model with $\omega_p^{\text{Ag}} = 2175 \text{ THz}$ and $\omega_r^{\text{Ag}} = 4.35 \text{ THz}$.

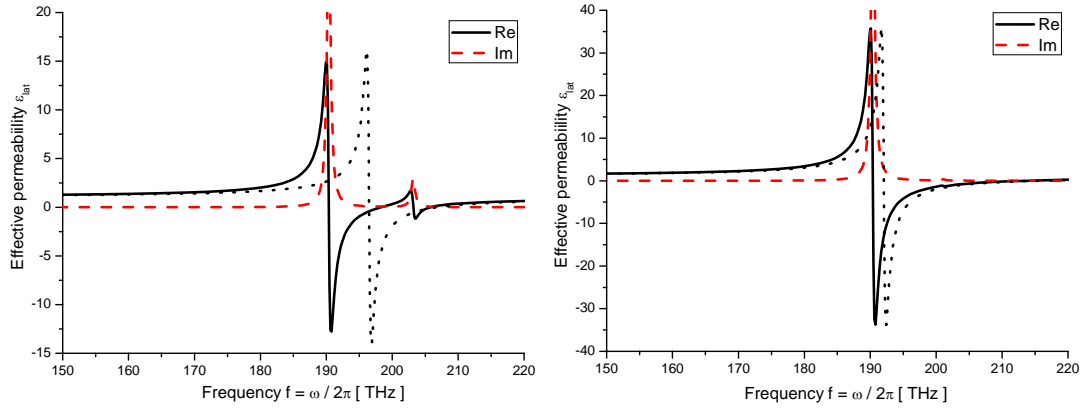


Fig. 3 – Effective relative electric permittivity $\varepsilon_{\text{eff}}^{(p)} / \varepsilon_0$ for the bulk media with the parameters of Fig. 2a and 2b. The dot-lines represent the effective permittivity of another bulk medium that could be formed by embedding the same number density of silver nanospheres as in the simulations, but in a regular periodic cubic lattice, not collected in loop arrangement.

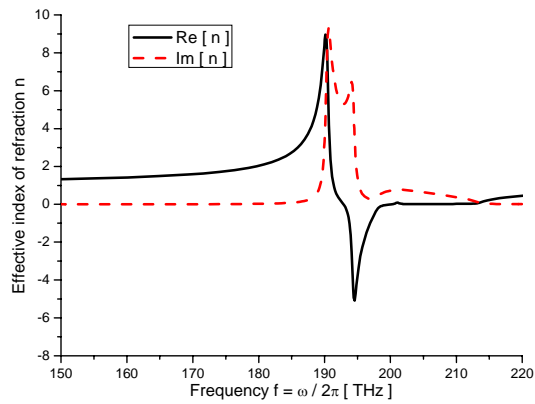


Fig. 4 –Effective index of refraction for the material composed as in Fig. 2b and 3b.

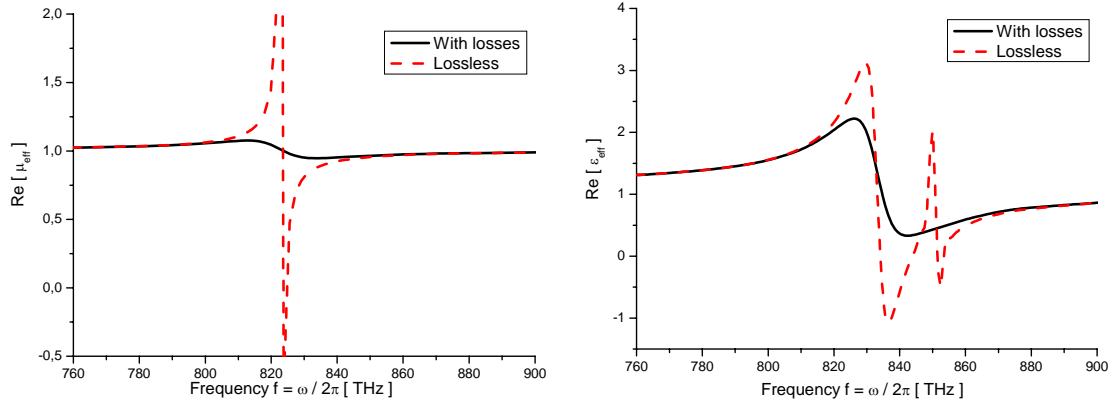


Fig. 5 – Real parts of: (a) the effective magnetic permeability $\mu_{\text{eff}}^{(p)} / \mu_0$, and (b) effective electric permittivity $\varepsilon_{\text{eff}}^{(p)} / \varepsilon_0$, for the following parameters: $R = 31.5 \text{ nm}$, $a = 10.5 \text{ nm}$, $N = 6$, $N_d = (95 \text{ nm})^{-3}$. The constitutive parameters here have been derived by interpolating the experimental data from [13] in the visible regime.

REFERENCES

- [1] R. W. Ziolkowski, and E. Heyman, Phys. Rev. E, **64**, 056625 (2001).
- [2] R. A. Shelby, D. R. Smith, and S. Schultz, Science, **292**, 77 (2001).
- [3] L. Landau, and E. M. Lifschitz, *Electrodynamics of continuous media* (Elsevier, 1984).
- [4] V. A. Podolskiy, A. K. Sarychev, and V. M. Shalaev, J. Nonlin. Opt. Phys. Mat., **11**, 65 (2002).
- [5] S. O'Brien, D. McPeake, S. A. Ramakrishna, and J. B. Pendry, Phys. Rev. B, **69**, 241101 (2004).
- [6] G. Shvets, and Y. A. Urzhumov, Phys. Rev. Lett., **93**, 243902 (2004).
- [7] M. L. Povinelli, S. G. Johnson, J. D. Joannopoulos, and J. B. Pendry, Appl. Phys. Lett., **82**, 1069 (2003).
- [8] A. Ishimaru, *et al.*, IEEE Trans. Antennas Propag., **51**, 10, 2550 (2003).
- [9] J. D. Jackson, *Classical Electrodynamics* (Wiley, 1998).

- [10] C. F. Bohren, and D. R. Huffman, *Absorption and Scattering of Light by Small Particles* (Wiley, New York, 1983).
- [11] S. Tretyakov, *Analytical Modeling in Applied Electromagnetics* (Artech House, 2003).
- [12] I. El-Kady, M. M. Sigalas, R. Biswas, K. M. Ho, and C. M. Soukoulis, Phys. Rev. B, **62**, 15299 (2000).
- [13] P. B. Johnson, and R. W. Christy, Phys. Rev. B, **6**, 4370 (1972).